Hydrol. Earth Syst. Sci. Discuss., 10, 15871–15914, 2013
www.hydrol-earth-syst-sci-discuss.net/10/15871/2013/
doi:10.5194/hessd-10-15871-2013

Hydrology and Earth System Sciences
Open Access
Discussions

Understanding mean transit times in Andean tropical montane cloud forest catchments: combining tracer data, lumped parameter models and uncertainty analysis

E. Timbe[1,2], D. Windhorst[2], P. Crespo[1], H.-G. Frede[2], J. Feyen[1], and L. Breuer[2]

[1]Departamento de Recursos Hídricos y Ciencias Ambientales, Dirección de Investigación (DIUC), Universidad de Cuenca, Cuenca, Ecuador
[2]Institute for Landscape Ecology and Resources Management (ILR), Research Centre for Bio Systems, Land Use and Nutrition (IFZ), Justus-Liebig-Universität Gießen, Gießen, Germany

Received: 27 November 2013 – Accepted: 3 December 2013 – Published: 23 December 2013

Correspondence to: E. Timbe (edison_timbe@yahoo.com)

Published by Copernicus Publications on behalf of the European Geosciences Union.

Abstract

Weekly samples from surface waters, springs, soil water and rainfall were collected in a 76.9 km^2 mountain rain forest catchment and its tributaries in southern Ecuador. Time series of the stable water isotopes δ^{18}O and δ^2H were used to calculate mean transit times (MTTs) and the transit time distribution functions (TTDs) solving the convolution method for seven lumped parameter models. For each model setup, the Generalized Likelihood Uncertainty Estimation (GLUE) methodology was applied to find the best predictions, behavioral solutions and parameter identifiability. For the study basin, TTDs based on model types such as the Linear-Piston Flow for soil waters and the Exponential-Piston Flow for surface waters and springs performed better than more versatile equations such as the Gamma and the Two Parallel Linear Reservoirs. Notwithstanding both approaches yielded a better goodness of fit for most sites, but with considerable larger uncertainty shown by GLUE. Among the tested models, corresponding results were obtained for soil waters with short MTTs (ranging from 3 to 12 weeks). For waters with longer MTTs differences were found, suggesting that for those cases the MTT should be based at least on an intercomparison of several models. Under dominant baseflow conditions long MTTs for stream water ≥ 2 yr were detected, a phenomenon also observed for shallow springs. Short MTTs for water in the top soil layer indicate a rapid exchange of surface waters with deeper soil horizons. Differences in travel times between soils suggest that there is evidence of a land use effect on flow generation.

1 Introduction

The mean transit time (MTT) of waters provides a valuable primary description of the hydrologic (Fenicia et al., 2010) and biochemical systems (Wolock et al., 1997) of a catchment and its sensitivity to anthropogenic factors (Landon et al., 2000; Turner et al., 2006; Tetzlaff et al., 2007; Darracq et al., 2010). The transit time distribution

HESSD
10, 15871–15914, 2013

function (TTD) describes the probability that water was at some point in the catchment a given amount of time ago (McDonnell et al., 2010). Together with the physical characteristics of the catchment, the MTT and TTD allow inferring the recharge of aquifers (Rose et al., 1996), the bulk water velocities through its compartments (Rinaldo et al., 2011), and the interpretation of the water chemistry (Maher, 2011); all of which supports the design of prevention, control, remediation and restoration techniques. Additionally, MTT and TTD data are useful to reduce the uncertainty of results and improve input parameter identifiability for either hydrologic modeling studies (Weiler et al., 2003; Vache and McDonnell, 2006; McGuire et al., 2007; Capell et al., 2012) or solute movement analyses through soil and aquifers using mixing models (Iorgulescu et al., 2007; Barthold et al., 2010).

The stable water isotopes $\delta^{18}O$ and $\delta^{2}H$ are commonly used as environmental tracers for a preliminary assessment of the transport of water in watersheds with transit times less than 5 yr (Soulsby et al., 2000, 2009; Rodgers et al., 2005; Viville et al., 2006). For longer MTTs, up to 12 yr, tritium radioisotopes are used to analyze the storage and flow behavior in surface water and shallow groundwater systems (Kendall and McDonnell, 1998), while carbon isotopes are employed for analyzing the dynamics of deep groundwater with ages of hundreds to thousands of years (Leibundgut et al., 2009).

Traditionally, researchers in tracer hydrology apply quasi distributed and conceptual models to encompass the non-linearity of the processes related to the transit states of the soil moisture dynamics (Botter et al., 2010; Fenicia et al., 2010). However, the use of such modeling approaches is only advisable after a basic inference of the MTTs using simpler TTDs as the lumped-parameter models proposed by Maloszewski and Zuber (1982, 1993), models that are based on quasi-linearity and steady state conditions. These models include the exponential (EM), piston (PM), or linear (LM) models, in which the MTT of the tracer is the only unknown variable, and also combinations of models such as the exponential-piston flow (EPM) and the linear-piston flow (LPM) models. Among the two-parameter lumped models, the dispersion model (DM), that

HESSD
10, 15871–15914, 2013

considers simplifications of the general advection-dispersion equation, has been applied in environmental tracer studies (Maloszewski et al., 2006; Viville et al., 2006; Kabeya et al., 2006). More recently, new lumped models are being exploited such as the two parameter Gamma model (GM) proposed by Kirchner et al. (2000), which is a more general and flexible version of the exponential model; and the Two Parallel Linear Reservoirs model (TPLR), a three-parameter function that combines two parallel reservoirs, each one represented by a single exponential distribution (Weiler et al., 2003). The use of these models for estimating the MTT in the compartments of a catchment has become a standard practice for the preliminary assessment of the catchment functioning. McGuire and McDonnell (2006) presented in their study a compilation of the most frequently used lumped parameter models for deriving MTTs. Under the condition that a particular model ought to be concordant with the physical characteristics of the aquifer system, this condition hinders the applicability of lumped parameter models to poor gauged catchments with scarce or no information on the physical characteristics of the system. For these cases the authors believe that it is better to use an ensemble of models in order to be certain that the results or the inferences point in the same direction, or if not, to have a better idea of the uncertainties. In accordance, seven lumped parameter models to infer the MTTs for diverse water stores (stream, springs, creeks and soil water) were applied in this study. Results were evaluated on the basis of the best matches to a predefined objective function, their magnitude of uncertainty and the number of observations in the range of behavioral solutions.

Particular for tropical zones the knowledge of hydrological functioning is still limited and investigation of system descriptors such as MTT and TTD are keys to improve our understanding of catchment responses (Murphy and Bowman, 2012; Brehm et al., 2008). This is especially the case for tropical mountain rainforest systems. In this study we focus on the San Francisco river basin, a mesoscale headwater catchment of the Amazon in Ecuador. Notwithstanding the recent characterization of the climate (Bendix et al., 2006), soils (Wilcke et al., 2002), water chemistry (Buecker et al., 2011) and hydrology (Plesca et al., 2012) of the basin, we are still lacking a perceptual model that

HESSD
10, 15871–15914, 2013

explains the observations of chemical, hydrometric and isotopic variables and related processes (Crespo et al., 2012).

To enhance the understanding of the hydrological functioning of the San Francisco basin, this study focuses on the (i) estimation of the MTT in the different compartments of the catchment; (ii) characterization of the dominant TTD functions; and (iii) evaluation of the performance and uncertainty of the models used to derive the MTTs and TTDs. Translated into hypotheses the study reported in this paper aimed to confirm or reject, respectively, that

1. the used tracers are conservative, there are no stagnant flows in the system, and the tracer mean transit time τ represents the MTT of water;
2. stationary conditions are dominant in the basin and lumped equations based on linear or quasi-linear behaviors are applicable;
3. given the steepness of the topography and the shallow depth of the soil layers the transit times of the sampling sites are less than 5 yr, making it possible to use δ^2H and δ^{18}O as tracers;
4. the diversity of the sampling sites allows evaluating the spatial variability in catchment hydrology, identifying the dominant processes, and screen the performance of the TTD models;
5. the multi-model approach and the identifiability of their parameters enable identification of the respective TTDs and MTTs.

2 Materials and methods

2.1 Study area

The San Francisco tropical mountain cloud forest catchment, 76.9 km^2 in size, is located in the foothills of the Andean cordillera in South Ecuador, between Loja and

HESSD
10, 15871–15914, 2013

Zamora (Fig. 1), and drains into the Amazonian river system. Hourly meteorological data recorded at the Estación Científica San Francisco (ECSF, 1957 m a.s.l.), El Tiro (2825 m a.s.l.), Antenas (3150 m a.s.l.) and TS1 (2660 m a.s.l.) climate stations are available from the DFG funded Research Unit FOR816 (www.tropicalmountainforest.org). Monthly averages of the main meteorological parameters for the period 1998–2012 allow a description of their spatial and interannual variation. Mean annual temperature ranges from 15 °C in the lower part of the study area (1957 m a.s.l.) to 10 °C on the ridge (3150 m a.s.l.), with an altitude gradient of −0.57 °C per 100 m, without marked monthly variability. The wind velocities of the prevailing south-easterlies reach average maximum daily values of 10 $m\,s^{-1}$ between June and September, while wind velocities in the middle and lower catchment areas are fairly constant, equal to 1 $m\,s^{-1}$. The humid regime of the catchment is comparatively constant with the relative humidity varying between 84.5 % in the lower parts and 95.5 % at the ridges. Among all meteorological parameters, precipitation shows the largest spatial variability, with an average gradient of 220 mm per 100 m^{-1} (Bendix et al., 2008b). However, this gradient is not constant throughout the catchment and shows substantial spatial variability (Breuer et al., 2013). Recent estimation of horizontal rainfall revealed its significance, contributing 5–35 % of measured tipping bucket rainfall, respectively to the lower and ridge areas of the catchment (Rollenbeck et al., 2011). Rainfall is marked by low rainfall intensities, generally less than 10 $mm\,h^{-1}$ and high spatial variability. Annual rainfall is uni-modal distributed with a peak in the period April–June. Using the Thiessen method and considering horizontal rainfall, the precipitation depth amounted 2321 mm in the period August 2010–July 2011, and 2505 mm in the period August 2011–July 2012. A more detailed descriptions of the weather and climate of the study area is given in Bendix et al. (2008a).

In line with findings of Crespo et al. (2012) baseflow in the same area accounts for 85 % of the total volume runoff (Table 2), notwithstanding the rapid and marked response of flows to extreme rainfall events. In just a few hours peak discharge is several

HESSD
10, 15871–15914, 2013

times higher than baseflow (Fig. 2c), carrying considerable amounts of sediment and accompanied by drastic changes in the cross section.

Mayor soil types are Histosols associated with Stagnasols, Cambisols and Regosols, while Umbrisols and Leptosols are present to a lesser degree (Liess et al., 2009). The geology is reasonable similar throughout the study area, consisting of sedimentary and metamorphic Paleozoic rocks of the Chiguinda unit with contacts to the Zamora batholith (Beck et al., 2008). The topography is characterized by steep valleys with an average slope of 63 %, situated in the altitudinal range of 1725–3150 m a.s.l. (Table 2). Protected by the Podocarpus National Park, the southern part of the catchment is covered by pristine primary forest and sub-páramo. In the northern part, particular during the last two decades, land is being converted to grassland. Presently 68 % of the catchment is covered by forest, 20 % is sub-páramo, 6.5 % is used as pasture and 3 % is degraded grassland covered with shrubs (Goettlicher et al., 2009; Plesca et al., 2012). Landslides are present in the catchment, especially along the paved road between the cities Loja and Zamora.

2.2 Catchment composition and discharge measurements

The San Francisco catchment is composed of seven sub-catchments with areas ranging between 0.7 and 34.9 km^2, characterized by different land uses varying from pristine forest and sub-páramo to pasture areas (Fig. 1 and Table 2). Since August 2010, water level and temperature sensors (mini-diver, Schlumberger Water Services, Delft, NL) with a 5 min resolution are installed at 4 tributaries of the catchment: FH, QN, QM, QC (Fig. 1) and in the main outlet (PL). As explained later in this section, specific discharges derived of these sites were used to account for the hydrological behavior of the remaining sub-catchments. In the QC cross section a 90° V-notch weir is installed for measuring the discharge. At PL a Doppler radar RQ-24 (Sommer Messtechnik, Koblach, AT) records water level and surface water velocity in 15 min resolution. Fortnightly, discharge is measured by the salt dilution method (Boiten, 2000) using portable electric conductivity probes (pH/cond 340i, WTW, Weilheim, DE) to develop

HESSD
10, 15871–15914, 2013

stage-discharge curves for each gauge station. The Manning method based on measurements of the wetted area and the stream velocity was used to complement and crosscheck manual measurements. For this purpose periodically the cross section in every gauge station was measured using a total station (SET650X, Sokkia, Olathe, Kansas, US). Figure 2 shows the hourly hydrograph for the main outlet (PL); similar hydrographs were calculated for the sections FH, QN, QC and QM.

2.3 Isotope sampling and analyses

Weekly isotope data were collected in the main river, its tributaries, creeks and springs in the period August 2010–mid August 2012 (Table 1), using 2 mL amber glass bottles. Soil water was sampled in the lower part of the catchment along two altitudinal transects covered by pasture and forest, respectively in 6 sites and 3 depths (0.10, 0.25 and 0.40 m) using wick-samplers. The soil water collectors were designed and installed as described by Mertens et al. (2007). Woven and braided 3/8 fiberglass wicks (Amatex Co. Norristown, PA, US) were unraveled over a length of 0.75 m and spread over a 0.30 m × 0.30 m × 0.01 m square plastic plate. The plate enveloped with fiberglass was covered with fine soil particles of the parent material and then set in contact with the undisturbed soil, respectively at the bottom of the organic horizon (0.10 m below surface), a transition horizon (0.25 m below surface) and a lower mineral horizon (0.40 m below surface). The low constant tension in the wick-samplers guarantees that the mobile phase of the soil water is sampled, avoiding isotope fractionation (Landon et al., 1999). Event based rainfall samples for isotope analyses were collected from mid-August 2010 until mid-August 2012, in an open area (1900 m a.s.l.) at ECSF (Fig. 1). The end of a single rainfall event was marked by a time span of 30 min without rainfall.

The stable isotopes signatures of $\delta^{18}O$ and $\delta^{2}H$ are reported in per mil relative to the Vienna Standard Mean Ocean Water (VSMOW) (Craig, 1961). The water isotopic analyzes were performed using a compact wavelength-scanned cavity ring down spectroscopy based isotope analyzer (WS-CRDS) with a precision of 0.1 per mil for $\delta^{18}O$ and 0.5 for $\delta^{2}H$ (Picarro L1102-i, CA, US).

HESSD
10, 15871–15914, 2013

2.4 Isotopic gradient of rainfall

Given the large altitudinal gradient in the San Francisco basin, it is to be expected that the input isotopic signal of rainfall for every sub-catchment varies according to its elevation (Dansgaard, 1964). In this regard, Windhorst et al. (2013) estimated this variation for the main transect of the catchment: −0.22 ‰ δ^{18}O, −1.12 ‰ δ^{2}H and 0.6 ‰ deuterium excess per 100 m elevation gain. Applying this altitude gradient under the assumption that the incoming rainfall signal is the sole source of water, thereby excluding any unlikely source of water from outside the topographic catchment boundaries with a different isotope signal, it was possible to derive the recharge elevation and localized input signal in each sub-catchment. The derived recharge elevations were used to crosscheck that they are inside the topographic boundaries of every sub-catchment (Table 5) and comparable to their mean elevations (Table 2).

Since no marked fractionation was observed for all analyzed waters it is highly probable that similar estimations of MTT are derived using either δ^{18}O or δ^{2}H (Fig. 3). Therefore, in this study δ^{18}O was selected for further analysis.

2.5 Mean transit time estimation and transit time distribution

Mean transit times were calculated based on stationary conditions. In the case of stream water this condition was fulfilled by considering only baseflow conditions (Heidbüchel et al., 2012), which were dominant in the catchment during the 2 yr observation period, accounting for 85 % of total runoff volume. Baseflow separations for streamflow were obtained through parameter fitting to the slope of the recessions in the observed hourly flows using the Water Engineering Time Series PROcessing tool (WETSPRO), developed by Willems (2009). To account for samples taken at baseflow conditions in sites where hydrometric records were not available, the specific discharges of the closer catchments with similar characteristics in terms of land use, size, and observed hydrologic behavior were used. In this sense, QZ, QR and QP were considered similar

HESSD
10, 15871–15914, 2013

to QN, QM and QC (Table 2). Soil and spring waters are less influenced by particular rain events and therefore all samples were included in the analysis.

For the calculation of MTTs, the authors used the lumped parameter approach. In this, the aquifer system is treated as an integral unit and the flow pattern is assumed to be constant as outlined in Maloszewski and Zuber (1982) for the special case of constant tracer concentration in time-invariant systems. In this case the transport of a tracer through a catchment is expressed mathematically by the convolution integral. The tracer output $C_{out}(t)$ and input $C_{in}(t)$ are related in function of time:

$$C_{out}(t) = \int_{-\infty}^{t} C_{in}(t') \exp\left[-\lambda(t-t')\right] g(t-t')\mathrm{d}t' \quad (1)$$

In the convolution integral, the stream outflow composition C_{out} at a time t (time of exit) consists of a tracer C_{in} that falls uniformly on the catchment in a previous time step t' (time of entry), C_{in} becomes lagged according to its transit time distribution $g(t-t')$; the factor $\exp[-\lambda(t-t')]$ is used to correct for decay if a radioactive tracer is used (λ = tracer's radioactive decay constant). For stable tracers ($\lambda = 0$), and considering that the time span $t-t'$ is the tracer's transit time τ, the Eq. (1) can be simplified and re-expressed as:

$$C_{out}(t) = \int_{-\infty}^{t} C_{in}(t') g(\tau)\mathrm{d}t' \quad (2)$$

where the weighting function $g(\tau)$ or tracer's transit time distribution (TTD), describes the normalized distribution function of the tracer injected instantaneously over an entire area (McGuire and McDonnell, 2006). As it is hard to obtain this function by experimental means, the most common way to apply this lumped approach is to adopt a theoretical distribution function that better fits to the studied system. In general meaning, any type of a weighting function is understood as a model. The equations for each of

HESSD
10, 15871–15914, 2013

the lumped parameter models used in this study are shown in Table 3. EM and LM reflect simpler transitions where the tracer's mean transit time τ is the only unknown variable. More flexible models consider a mixture of two different types of distribution. EPM includes piston and exponential flows, while the LPM accounts for piston and linear flows. In both cases the equations are integrated by the parameter η indicating the percentage contribution of each flow type distribution. The DM, derived from the general equation of advection-dispersion, is also one of the common models used in hydrologic systems (Maloszewski et al., 2006). In this model the fitting parameter D_p is related to the transport process of the tracer (Kabeya et al., 2006). In the GM, the product of the two shape parameters α and β equals τ. This method was successfully applied by Dunn et al. (2010) and Hrachowitz et al. (2010). The TPLR model (Weiler et al., 2003) is based on the parallel combination of two single exponential reservoirs (despite of its name TPLR follows exponential and not linear assumption), representing fast τ_f and slow flows τ_s, respectively. The flow partition between the two reservoirs is denoted by the parameter φ.

2.6 Convolution equation resolution

The conventional resolution of the convolution equation requires the continuity of data for each time step of the input function. Weekly data of the isotopic composition of all sampled waters were therefore used in this study. Available sub-daily rainfall data were weighed according to the daily volume registered at the nearest meteorological station (ECSF, Figs. 1 and 2a). For the 2 yr sampling period, only 5 weeks without rainfall were registered. For these cases, average values considering the antecedent and precedent weekly isotopic signatures were used.

Due to the similarities between the seasonal isotopic fluctuations of the sampled effluents and rainfall signal, a constant interannual recharge of the aquifers was assumed. For each sampling site, the 2 yr isotopic data series were used as input for the models. To get stable results between two consecutive periods, these input isotope time series were repeated 20 times in a loop; an approach similar to the methodology

HESSD
10, 15871–15914, 2013

presented by Munoz-Villers and McDonnell (2012) resulting in an artificial time series of 40 yr. Data of the last loop were considered for statistical treatment and analysis. The repetition of the input isotopic signal implies that interannual variation of rain is negligible; an acceptable assumption for the San Francisco catchment considering the high degree of similarity between the same months along the analyzed 2 yr period (Fig. 4). Comparable monthly isotopic seasonality of rainfall has been described by Goller et al. (2005) for the same study area and for nearby regions with similar climatic conditions, e.g., Amaluza GNIP station (http://www.iaea.org/water).

2.7 Evaluation of model performance

The search for acceptable model parameters for each site was conducted through statistical comparisons of 10 000 simulations based on the Monte-Carlo method, considering a uniform random distribution of the variables involved in each model. For each site and model its performance was calculated using the Nash–Sutcliffe Efficiency (NSE). Quantification of errors and deviations from the observed data were respectively calculated by the root mean square error (RMSE) and the bias. MatLab version 7 was used for data handling and solving the convolution equation.

The Generalized Likelihood Uncertainty Estimation (GLUE, Beven and Freer, 2001), was used to find uncertainty ranges of possible or behavioral parameter solutions. The GLUE approach considers that several likely solutions are valid as long as efficiency of a particular simulation is above a pre-set, but subjective threshold. Due to the diversity of sampling sites, multiple models and the expected range of variability for NSE among sites, a fixed confidence interval of 5–95 % of the top 5 % of the best NSE was applied as a lower threshold for every case. Besides, a prediction was considered poor whenever the best NSE was below 0.45.

The following three criteria were used to select the best solutions of MTTs and TTDs: (1) NSE; (2) magnitude of the uncertainty of the prediction, expressed as a percent of the predicted MTT value; and (3) percentage of observations covered by the range of behavioral solutions defined according to the second criteria.

HESSD
10, 15871–15914, 2013

3 Results

3.1 Soil water

Of all predictions the best matches of the models with respect to the NSE objective function ranged between 0.64 and 0.91 (Fig. 5a). When only the best goodness of fit is considered, the GM and the EPM models performed best in 13 of the 18 sampled sites, the DM model in 3 sites, and the LM and LPM models in one location (Fig. 5b). Only these models were considered for further mutual comparison. The TPLR and EM approaches performed worst in 17 of the 18 sites (Fig. 5a), and were therefore not further considered. Even when the derived MTT values were similar among the models that best fitted the objective function (Fig. 6a), the LPM model performed best taking into consideration additional selection criteria, as shown in Fig. 6b and c. Figure 8 depicts for the LPM model, applied to site C2, the uncertainty and the range of behavioral solutions for the two model parameters. Uncertainties, expressed on average values for all soil sites (Fig. 6b), were lower for LM (32 %), LPM (35 %) and GM (37 %) models than for DM (51 %) and EPM (44 %) models. The percentage of observations described inside the range of behavioral solutions according to their uncertainty ranges (Fig. 6c) was bigger for LPM (68 %) and EPM (59 %) models compared to the DM (47 %), GM (41 %) and LM (33 %) models.

According to the standard deviations (σ) of the observed $\delta^{18}O$, the amplitude of seasonality between sites and horizons, varied from 2.57 to 3.98 ‰ (Table 4), very similar to the σ of weekly rainfall data (4.3 ‰). Except for the A3 and D2 sites, σ showed a decreasing pattern according to the sampling depth. Besides, they are inverse linearly correlated to the estimated MTTs (for LPM model results were $\tau = -2.4474\sigma + 12.954, r^2 = 0.60$), indicating a distinctive decrease in the pattern of MTT with soil depth (0.10, 0.25 and 0.40 m).

Considering results from the LPM model (Table 4), differences between observed and predicted values described by the RMSE are up to 1.72 ‰ and the larger absolute bias accounts for 0.181 ‰ (Table 4). Bearing in mind the ranges of behavioral solution,

HESSD
10, 15871–15914, 2013

MTT results were between 2.3 and 6.3 weeks for pastures soils and between 3.7 and 9.2 weeks for forested soils, while parameterizations for η (ratio of the total volume to the volume in which linear flow applies) ranged from 0.84 to 2.23 and from 0.76 to 1.61 respectively.

3.2 River and tributaries

Considering all sites and models the criteria NSE > 0.45 was exceeded in 41 of the 63 predictions (9 sites per 7 models, Fig. 5a). Among the analyzed sites the TPLR model yielded the best matches for PL, SF, FH, QZ, QN, QM and QC, while the EPM model for the QR and QP sites (Fig. 5b). The GM model reached closest efficiencies when compared to the best match for every site. Consequently only the TPLR, EPM and GM models were further considered. Although the best NSEs were reached using the TPLR model (0.61 on average for all sites) compared to the GM (0.57 on average) or the EPM (0.55 on average) model, TPLR predictions showed the largest uncertainties (115 % on average of predicted MTTs, Fig. 7b) and at the same time depicted the lowest number of observations inside the predicted range of behavioral solutions (29 % on average, Fig. 7c). Considering these additional selection criteria, EPM performed better: uncertainty of MTT was on average 16 % (66 % on average for GM model) and the number of observation inside this range was 72 % (33 % on average for GM model). Differences between MTT predictions for a particular site are depicted in Fig. 7a. For stream water at the main outlet, Figs. 9–11 show the parameter uncertainties and behavioral solutions for the TPLR, GM and EPM models, respectively.

Considering the results from the EPM model (Table 5, Fig. 7a), the low seasonal amplitudes described by the observed data of the effluents (σ between 0.30 and 0.59 ‰) resulted in small errors and deviations when simulated and observed data were compared (RMSE up to 0.41 ‰ and larger absolute bias of 0.005 ‰). But at the same time, the fitting efficiencies were lower than for soil waters, with a maximum NSE of 0.56 for the main stream, and NSEs between 0.48 and 0.58 for the main tributaries (Fig. 5a). The predicted MTT at catchment outlet was 2.0 yr with a η parameter of 1.84

HESSD
10, 15871–15914, 2013

(a similar value was estimated for the main river at the SF sampling site, MTT = 2.0 yr and η = 1.85) and varied from 2.0 (QM, η = 1.85) to 3.9 yr (QC, η = 1.97) for the main tributaries. As in the case of water from soils, results of MTT followed an inverse linear correlation with amplitude of observed data (σ): $\tau = -7.3152\sigma + 5.9893$; $r^2 = 0.91$. Independent of the amplitude of the isotope signal between sampled sites (σ), uncertainties for each site were similar with a maximum range between 14.1 % and 20.4 % of the predicted MTT as derived for the FH and QM sites (Table 5). Similarly, η ranged from 1.61 (QZ) to 2.21 (QP), the average value of η = 1.85 implies a 54 % of volume portion of exponential flow and a 46 % volume of piston flow; the uncertainty for the η parameter was 25 % on average.

3.3 Springs and creeks

Of 35 predictions (5 sites per 7 models) the criteria NSE > 0.45 was fulfilled in 20 cases. Sites with reduced isotope signal yielded lower efficiencies (Fig. 5a); i.e. for the TP site only two models provided NSE values higher than 0.45: EPM (NSE = 0.49) and TPLR (NSE = 0.51). For the QRS site only the DM model (NSE = 0.68) qualified, while for the remaining sites the criteria NSE > 0.45 was reached at least by 5 models. Except for the QRS site, the remaining sites showed similarities to stream waters in the sense of best models to describe the data when only the best fits to the objective function were considered: TP, PLS and SFS sites were best described using a TPLR distribution function while Q3 was best described by a GM distribution. GM was also the second best model for the PLS and SFS sites. At the same time, EPM was the second best model for the TP site and the third one for the Q3 and PLS sites. The DM model performed best only for the QRS site (Fig. 5a). As for stream waters, when comparing the EPM model to the TPLR or GM models (Fig. 7), this one performed best when considering two additional selection criteria: an uncertainty equal or less than 17 % on the predicted MTTs (45 and 77 % for GM and TPLR models) and 73 % of observed data inside the range of behavioral solutions (27 % for GM or TPLR models).

HESSD
10, 15871–15914, 2013

Among the analyzed sites (detailed results are shown in Table 5), the amplitudes of observed $\delta^{18}O$ data described by σ, ranged from 0.25 to 0.54 ‰ for the small creeks TP and Q3; while values of 0.17, 0.29 and 0.50 ‰ for the springs QRS, SFS and PLS, respectively. Similar to stream water, the damped amplitudes yielded lower efficiencies than for soil waters but at the same time lower errors and bias. Considering EPM, MTTs of 4.5 yr (NSE = 0.49, η = 1.74) for TP and 2.1 yr (NSE = 0.65, η = 1.84) for Q3 were estimated; while for springs, 2.0 yr (NSE = 0.69, η = 1.85) for PLS and 3.3 yr (NSE = 0.47, η = 1.42) for SFS. Results for the QRS site showed poor reliability due to the reduced amplitude of $\delta^{18}O$ in the observed data, the lowest among the observed sites (σ = 0.17). For this site, using the EPM model a maximum NSE of 0.28 was reached, vs. an efficiency of 0.25 for the TPLR and GM models. Estimations for MTTs were larger than 5 yr, and therefore beyond the level of applicability of the method for natural isotopic tracers.

4 Discussion

For soil waters, similar MTT results of a few weeks to months were obtained regardless the lumped parameter models used (Fig. 6a). Although the LPM model did not yield predictions with the highest efficiencies, the predicted TTD yielded smaller ranges of uncertainty (Fig. 6b) and a larger number of observations inside them (Fig. 6c), advantages that could not be inferred by using only the best matches to NSE, for which GM and EPM models performed better than others (Fig. 5b). Using a LPM model, suitable to describe a partially confined aquifer with increasing thickness (Maloszewski and Zuber, 1982), we found MTTs varying from 2.3 to 6.3 weeks for pastures sites and from 3.7 to 9.2 weeks for forested soils. If we consider that only the top soil horizon was sampled (maximum sampled depth was 0.4 m), these results are comparable to values between 7.5 and 31 weeks found in 2.0 m soil columns of typical Bavarian soil using the DM model (Maloszewski et al., 2006).

HESSD
10, 15871–15914, 2013

For larger MTTs (> 1 yr), as derived for sampled surface waters and shallow springs, there were differences when predicted results among models were compared (Fig. 7a), especially for sites with strong damped signals of measured $\delta^{18}O$ (e.g. QRS and TP sites). Similarly to soil waters, when considering uncertainties, the EPM model performed significantly better when compared to the TPLR or GM models, although the latter two performed best for most of the sampled surface waters according to the NSE objective function (Fig. 5a and b).

When analyzing results from different models, dotty plots of model parameter uncertainty are very useful to display not only the magnitude of uncertainty but also its tendency. Similarly, the uncertainty bands of behavioral solutions can help to account for the sensitivity of the parameter uncertainty on $\delta^{18}O$ modeled results. For example, when predicted results for the PL site are compared, larger parameter uncertainty and skewness are notorious for TPLR than for EPM or GM models (Figs. 9a–c for TPLR, 10a–c for GM and 11a and b for EPM). At the same time EPM shows the highest sensitivity in modeled results (Figs. 9d, 10d, 11c). In order to contrast the signature of the effluent with younger waters such as rainfall, Figs. 9e, 10e, or 11d show the damped observed (and predicted) $\delta^{18}O$ signatures at the main outlet; a characteristic present in all analyzed surface waters. Considering the efficiencies reached by the predictions, we should keep in mind that ranges of behavioral solutions derived from a fixed 5 % of the top NSE are generally smaller than a predefined lower limit for all waters, e.g., a predefined lower efficiency limit of 0.30 and 0.45 were used by Speed et al. (2010) and Capell et al. (2012), respectively.

Considering the LPM results for MTTs of soil water from pastures (4.3 weeks on average) and forest sites (5.9 weeks on average) as independent data sets, a two tailed p value of 0.0075 for a Student's t test was calculated, meaning that the difference between the two groups was statistically significant, although physical characteristics, like length, slope and altitude and meteorological conditions of the respective hill slopes were more or less similar. Land use effects affecting soil hydraulic properties controlling the infiltration and flow of water were detected in previous studies within

HESSD
10, 15871–15914, 2013

the research area (Huwe et al., 2008). Confirming findings in other tropical catchments were published by Zimmermann et al. (2006), who stated that under grazing the hydraulic conductivity decreased, overland and near surface flows increased, the storage capacity of the soil matrix declined, with feedbacks on the MTT of soil water. Similar insights were found by Tetzlaff et al. (2007) comparing two small catchments in Central Scotland Highlands of different land use.

The variation range between the fitting efficiencies and corresponding results of MTTs for stream water among the 7 models for a given site was higher when compared to the ones for soil water. This was somehow to be expected, since the dampening effect on a catchment to sub-catchment scale generates a smoother signal filtering/averaging the heterogeneity observed at a single point along a precise transect. Since for most of the cases the calculated MTT for soil waters showed an increasing pattern according to soil depth, longer MTTs corresponding to longer distances to the stream were to be expected due to the seepage of water from the deeper soil layer. Soil water below 0.4 m was not monitored within this study, given the shallow soil depth and the increasing fraction of rock material with depth, preventing the use of wick samplers.

The similarities and differences between models for sites with MTTs > 1 yr, as for stream and spring waters, gave insights about the importance to account for a proper TTD, defined according to the conceptual knowledge of the catchment's functioning, before calculating MTT. In this regard, the use of a multi-model approach and uncertainty analysis is believed essential as to be able of defining which functions describes in a better way the parameter identifiability and bounds of behavioral solutions. By considering best matches to NSE for stream waters, best predictions were obtained with the TPLR, EPM and GM models; being more flexible versions of a pure exponential distribution function (i.e. EM model) that helps to account for non-linearities of the system. The same distribution functions were identified as good predictors of observed data in a related study by Weiler et al. (2003). Nevertheless, the damped isotopic signal of all surface and spring waters compared to the rainfall input function provided lower efficiencies of predictions than for soil waters. Among these models and considering

HESSD
10, 15871–15914, 2013

the uncertainties of the estimations, EPM can be considered the most reliable for the surface waters of the San Francisco catchment. When comparing the TPLR to EPM or GM models, the latter two take the non-linearity of the flow without splitting it in two reservoirs with different exponential behaviors into account, therefore yielding more identifiable results. Larger uncertainties for the TPLR three parameter model was also found by Hrachowitz et al. (2009b). However, findings by Weiler et al. (2003) suggest that the TPLR distribution function could achieve better predictions for runoff events generated by mixed fast and slow flows. On the other hand, in related studies the EPM model yielded better predictions for surface and spring waters (Viville et al., 2006). In the San Francisco catchment, the average $\eta = 1.85$ value for surface waters (similar values were found for creeks: $\eta = 1.79$ and springs: $\eta = 1.64$) implies that a significant portion of old water (46 %) is released previous to the new one (54 %). The η value in this study is larger than the η value found in studies for stream water in temperate small headwaters catchments ($\eta = 1.09$, Kabeya et al., 2006; $\eta = 1.28$, McGuire et al., 2002; $\eta = 1.37$, Asano et al., 2002), and close to results published by Katsuyama et al. (2009) for two riparian groundwater systems ($\eta = 1.6$ and 1.7).

The Gamma model, identified as the second best model for surface waters and springs in the San Francisco catchment, was also identified as an applicable distribution function in headwater montane catchments with dominant baseflow in temperate climate (Hrachowitz et al., 2009a, 2010; Dunn et al., 2010). For our study area, a characteristic shape parameter $\alpha < 1$ (e.g. Fig. 10b) was found in all stream and spring sites meaning that an initial peak or a significant part of the flow was quickly transported to the river. Similar results were found recently for mountain catchments of comparable size in Scotland by Kirchner et al. (2010), who also stated the importance for accounting the best distribution shape, which is usually assumed as purely exponential ($\alpha = 1$). MTTs derived without the use of observed data using a purely exponential model frequently led to an overestimation of α and consequently an underestimation of MTTs. The higher flexibility of the GM model permits to account for the non-linearity in the behavior of a catchment system (Hrachowitz et al., 2010).

HESSD
10, 15871–15914, 2013

5 Conclusions

The research revealed that looking for the best TTD and its derived MTT is not only matter of accounting for the best fit to a predefined objective function, instead, it is recommended to (1) include in the analysis several potential TTD models, (2) assess the uncertainty range of predictions and (3) account for the parameter identifiability. Although the uncertainty range increases for MTTs larger than 1–2 yr, using simpler models that still yield acceptable fits to an objective function can help to reduce the uncertainty associated to the predictions. In this sense, using the best predictions from models like LPM for soil waters and EPM for surface and spring waters yielded a more reliable range of MTT inferences through lowering the uncertainty associated in the predictions of certain models. Sites that showed substantial differences in predictions between models (e.g. QRS or TP) were related to a strong reduction of the isotopic signal yielding larger uncertainties and extended MTT predictions getting close to the limitations of the used method. It is recommended to interpret these results with care, even to not consider them until longer time series of isotopic data are available.

The diversity of sampling sites and uncertainty analysis, based on the best fits to the objective function NSE and the identifiability of the parameters of the convolution equations of 7 conceptual models, allowed to define with adequate accuracy the ranges of variation of the mean transit times (MTTs) and the proper distributions functions (TTDs) for the main hydrological compartments of the San Francisco catchment. Pure exponential distributions (i.e. EM) provided the poorest predictions in all sites, suggesting non-linearities of the processes, as produced by preferential or bypass flow. On the other hand, models such as EPM or GM which have a better performance in terms of considering the non-linearity, in most cases yielded better fits to the observed data and at the same time better identifiability of its variables (τ, η or α).

For baseflow conditions, which are annually dominant in the catchment area, stream water at the main outlet (PL) and five tributaries (FH, QZ, QN, QR, QM) yielded similar MTT estimations, ranging from 1.8 to 2.5 yr, including uncertainty ranges; while

HESSD
10, 15871–15914, 2013

the MTT estimation for two tributaries (QP and QC) were between 3.5 and 4.4 yr. Despite the similar contribution areas, 2 small creeks described contrasting transit times, TP between 4.2 and 5.1 yr, and Q3 between 1.9 and 2.2 yr. Springs showed a longer variation range, from 2.0 yr for PLS to larger than 5 yr for QRS. Considering the predominance of the stream water characteristics of the larger sub-catchments and the higher variability of smaller tributaries (creeks and springs), there is a clear indication that the heterogeneity of the small scale aquifers is averaged in large areas. In this sense, an in depth analysis on individual functioning or intercomparison between analyzed sites, which was beyond the scope of this paper, should be performed in selected areas using longer time series.

Two transects based on land cover characteristics showed differences in MTTs. Pastures have shorter ranges (2.3–6.3 weeks) than forested (3.7–9.2 weeks) areas. Considering the characteristics of the sampling sites (Table 2), results suggest a possible regulatory effect of land use on water movement. Although the representativeness of the sampled sites is low in comparison to the total catchment area, findings point out the potential of environmental tracer methods for estimating the effects of changes in vegetation, a task usually difficult to accomplish by conventional hydrometric methods.

Acknowledgements. The authors are very grateful for the support provided by Karina Feijo during the field sampling campaign which most of the times was conducted in harsh climatic conditions. Thanks are due to the German students spending throughout the research short-stays at the San Francisco Research Station helping with the realization of the aims of the project and more importantly for providing a friendly working environment. In this regard we like to acknowledge especially the dedication of Caroline Fries, Thomas Waltz and Dorothee Hucke. Furthermore, special thanks are due to Irene Cardenas for her unconditional support with the vast amount of lab analyses. Thanks are also due to Thorsten Peters of the University of Erlangen for providing meteorological data and the logistic support offered by Felix Matt and Jorg Zeilinger, and the administrative and technical staff of the San Francisco Research Station. Last but not least, the authors recognize that this research would not have been possible without the financial support of the German Research Foundation (DFG, BR2238/4-2) and the Secretaria Nacional de Ciencia, Tecnología e Innovación (SENESCYT).

HESSD
10, 15871–15914, 2013

References

Asano, Y., Uchida, T., and Ohte, N.: Residence times and flow paths of water in steep unchannelled catchments, Tanakami, Japan, J. Hydrol., 261, 173–192, doi:10.1016/S0022-1694(02)00005-7, 2002.

Barthold, F. K., Wu, J., Vache, K. B., Schneider, K., Frede, H.-G., and Breuer, L.: Identification of geographic runoff sources in a data sparse region: hydrological processes and the limitations of tracer-based approaches, Hydrol. Process., 24, 2313–2327, doi:10.1002/hyp.7678, 2010.

Beck, E., Makeschin, F., Haubrich, F., Richter, M., Bendix, J., and Valerezo, C.: The ecosystem (Reserva Biológica San Francisco), in: Gradients in a Tropical Mountain Ecosystem of Ecuador, edited by: Beck, E., Bendix, J., Kottke, I., Makeschin, F., and Mosandl, R., Springer, Berlin, 1–13, 2008.

Bendix, J., Homeier, J., Ortiz, E. C., Emck, P., Breckle, S.-W., Richter, M., and Beck, E.: Seasonality of weather and tree phenology in a tropical evergreen mountain rain forest, Int. J. Biometeorol., 50, 370–384, doi:10.1007/s00484-006-0029-8, 2006.

Bendix, J., Rollenbeck, R., Fabian, P., Emck, P., Richter, M., and Beck, E.: Climate variability, in: Gradients in a Tropical Mountain Ecosystem of Ecuador, edited by: Beck, E., Bendix, J., Kottke, I., Makeschin, F., and Mosandl, R., Springer, Berlin, 281–290, 2008a.

Bendix, J., Rollenbeck, R., Richter, M., Fabian, P., and Emck, P.: Climate, in: Gradients in a Tropical Mountain Ecosystem of Ecuador, edited by: Beck, E., Bendix, J., Kottke, I., Makeschin, F., and Mosandl, R., Springer, Berlin, 63–73, 2008b.

Beven, K. and Freer, J.: Equifinality, data assimilation, and uncertainty estimation in mechanistic modelling of complex environmental systems using the GLUE methodology, J. Hydrol., 249, 11–29, doi:10.1016/S0022-1694(01)00421-8, 2001.

Boiten, W.: Hydrometry, Taylor & Francis, The Netherlands, 2000.

Botter, G., Bertuzzo, E., and Rinaldo, A.: Transport in the hydrologic response: travel time distributions, soil moisture dynamics, and the old water paradox, Water Resour. Res., 46, W03514, doi:10.1029/2009WR008371, 2010.

Brehm, G., Homeier, J., Fiedler, K., Kottke, I., Illig, J., Nöske, N. M., Werner, F. A., and Breckle, S. W.: Mountain rain forests in southern Ecuador as a hotspot of biodiversity – limited knowledge and diverging patterns, in: Gradients in a Tropical Mountain Ecosystem of Ecuador, edited by: Beck, E., Bendix, J., Kottke, I., Makeschin, F., and Mosandl, R., Springer, Berlin, 15–23, 2008.

HESSD
10, 15871–15914, 2013

Breuer, L., Windhorst, D., Fries, A., and Wilcke, W.: Supporting, regulating, and provisioning hydrological services, in ecosystem services, biodiversity and environmental change, in: A Tropical Mountain Ecosystem of South Ecuador, edited by: Bendix, J., Beck, E., Bräuning, A., Makeschin, F., Mosandl, R., Scheu, S., and Wilcke, W., Springer, Berlin, 107–116, 2013.

Buecker, A., Crespo, P., Frede, H.-G., and Breuer, L.: Solute behaviour and export rates in neotropical montane catchments under different land-uses, J. Trop. Ecol., 27, 305–317, doi:10.1017/S0266467410000787, 2011.

Capell, R., Tetzlaff, D., Hartley, A. J., and Soulsby, C.: Linking metrics of hydrological function and transit times to landscape controls in a heterogeneous mesoscale catchment, Hydrol. Process., 26, 405–420, doi:10.1002/hyp.8139, 2012.

Craig, H.: Standard for reporting concentrations of deuterium and oxygen-18 in natural waters, Science, 133, 1833, doi:10.1126/science.133.3467.1833, 1961.

Crespo, P., Buecker, A., Feyen, J., Vache, K. B., Frede, H.-G., and Breuer, L.: Preliminary evaluation of the runoff processes in a remote montane cloud forest basin using mixing model analysis and mean transit time, Hydrol. Process., 26, 3896–3910, doi:10.1002/hyp.8382, 2012.

Dansgaard, W.: Stable isotopes in precipitation, Tellus, 16, 436–468, doi:10.1111/j.2153-3490.1964.tb00181.x, 1964.

Darracq, A., Destouni, G., Persson, K., Prieto, C., and Jarsjo, J.: Scale and model resolution effects on the distributions of advective solute travel times in catchments, Hydrol. Process., 24, 1697–1710, doi:10.1002/hyp.7588, 2010.

Dunn, S. M., Birkel, C., Tetzlaff, D., and Soulsby, C.: Transit time distributions of a conceptual model: their characteristics and sensitivities, Hydrol. Process., 24, 1719–1729, doi:10.1002/hyp.7560, 2010.

Fenicia, F., Wrede, S., Kavetski, D., Pfister, L., Hoffmann, L., Savenije, H. H. G., and McDonnell, J. J.: Assessing the impact of mixing assumptions on the estimation of streamwater mean residence time, Hydrol. Process., 24, 1730–1741, doi:10.1002/hyp.7595, 2010.

Goettlicher, D., Obregon, A., Homeier, J., Rollenbeck, R., Nauss, T., and Bendix, J.: Land-cover classification in the Andes of southern Ecuador using Landsat ETM plus data as a basis for SVAT modelling, Int. J. Remote Sens., 30, 1867–1886, doi:10.1080/01431160802541531, 2009.

HESSD
10, 15871–15914, 2013

Goller, R., Wilcke, W., Leng, M. J., Tobschall, H. J., Wagner, K., Valarezo, C., and Zech, W.: Tracing water paths through small catchments under a tropical montane rain forest in south Ecuador by an oxygen isotope approach, J. Hydrol., 308, 67–80, doi:10.1016/j.jhydrol.2004.10.022, 2005.

Heidbüchel , I., Troch, P. A., Lyon, S. W., and Weiler, M.: The master transit time distribution of variable flow systems, Water Resour. Res., 48, W06520, doi:10.1029/2011WR011293, 2012.

Hrachowitz, M., Soulsby, C., Tetzlaff, D., Dawson, J. J. C., Dunn, S. M., and Malcolm, I. A.: Using long-term data sets to understand transit times in contrasting headwater catchments, J. Hydrol., 367, 237–248, doi:10.1016/j.jhydrol.2009.01.001, 2009a.

Hrachowitz, M., Soulsby, C., Tetzlaff, D., Dawson, J. J. C., and Malcolm, I. A.: Regionalization of transit time estimates in montane catchments by integrating landscape controls, Water Resour. Res., 45, W05421, doi:10.1029/2008WR007496, 2009b.

Hrachowitz, M., Soulsby, C., Tetzlaff, D., Malcolm, I. A., and Schoups, G.: Gamma distribution models for transit time estimation in catchments: physical interpretation of parameters and implications for time-variant transit time assessment, Water Resour. Res., 46, W10536, doi:10.1029/2010WR009148, 2010.

Huwe, B., Zimmermann, B., Zeilinger, J., Quizhpe, M., and Elsenbeer, H.: Gradients and patterns of soil physical parameters at local, field and catchment scales, in: Gradients in a Tropical Mountain Ecosystem of Ecuador, edited by: Beck, E., Bendix, J., Kottke, I., Makeschin, F., and Mosandl, R., Springer, Berlin, 375–386, 2008.

Iorgulescu, I., Beven, K. J., and Musy, A.: Flow, mixing, and displacement in using a data-based hydrochemical model to predict conservative tracer data, Water Resour. Res., 43, W03401, doi:10.1029/2005WR004019, 2007.

Kabeya, N., Katsuyama, M., Kawasaki, M., Ohte, N., and Sugimoto, A.: Estimation of mean residence times of subsurface waters using seasonal variation in deuterium excess in a small headwater catchment in Japan, Hydrol. Process., 21, 308–322, doi:10.1002/hyp.6231, 2006.

Katsuyama, M., Kabeya, N., and Ohte, N.: Elucidation of the relationship between geographic and time sources of stream water using a tracer approach in a headwater catchment, Water Resour. Res., 45, W06414, doi:10.1029/2008WR007458, 2009.

Kendall, C. and McDonnell, J. J.: Isotope Tracers in Catchment Hydrology, Elsevier, Amsterdam, The Netherlands, 1998.

HESSD
10, 15871–15914, 2013

Kirchner, J. W., Feng, X. H., and Neal, C.: Fractal stream chemistry and its implications for contaminant transport in catchments, Nature, 403, 524–527, doi:10.1038/35000537, 2000.
Kirchner, J. W., Tetzlaff, D., and Soulsby, C.: Comparing chloride and water isotopes as hydrological tracers in two Scottish catchments, Hydrol. Process., 24, 1631–1645, doi:10.1002/hyp.7676, 2010.
Landon, M. K., Delin, G. N., Komor, S. C., and Regan, C. P.: Comparison of the stable-isotopic composition of soil water collected from suction lysimeters, wick samplers, and cores in a sandy unsaturated zone, J. Hydrol., 224, 45–54, doi:10.1016/S0022-1694(99)00120-1, 1999.
Landon, M. K., Delin, G. N., Komor, S. C., and Regan, C. P.: Relation of pathways and transit times of recharge water to nitrate concentrations using stable isotopes, Ground Water, 38, 381–395, doi:10.1111/j.1745-6584.2000.tb00224.x, 2000.
Leibundgut, C., Maloszewski, P., and Külls, C.: Environmental tracers, in: Tracers in Hydrology, John Wiley & Sons, Ltd., Chichester, UK, 13–56, doi:10.1002/9780470747148.ch3, 2009.
Liess, M., Glaser, B., and Huwe, B.: Digital soil mapping in southern ecuador, Erdkunde, 63, 309–319, doi:10.3112/erdkunde.2009.04.02, 2009.
Maher, K.: The role of fluid residence time and topographic scales in determining chemical fluxes from landscapes, Earth Planet. Sci. Lett., 312, 48–58, doi:10.1016/j.epsl.2011.09.040, 2011.
Maloszewski, P. and Zuber, A.: Determining the turnover time of groundwater systems with the aid of environmental tracers, 1. models and their applicability, J. Hydrol., 57, 207–231, 1982.
Maloszewski, P. and Zuber, A.: Principles and practice of calibration and validation of mathematical-models for the interpretation of environmental tracer data, Adv. Water Resour., 16, 173–190, doi:10.1016/0309-1708(93)90036-F, 1993.
Maloszewski, P., Maciejewski, S., Stumpp, C., Stichler, W., Trimborn, P., and Klotz, D.: Modelling of water flow through typical Bavarian soils: 2. environmental deuterium transport, Hydrol. Sci. J.-J. Sci. Hydrol., 51, 298–313, doi:10.1623/hysj.51.2.298, 2006.
McDonnell, J. J., McGuire, K., Aggarwal, P., Beven, K. J., Biondi, D., Destouni, G., Dunn, S., James, A., Kirchner, J., Kraft, P., Lyon, S., Maloszewski, P., Newman, B., Pfister, L., Rinaldo, A., Rodhe, A., Sayama, T., Seibert, J., Solomon, K., Soulsby, C., Stewart, M., Tetzlaff, D., Tobin, C., Troch, P., Weiler, M., Western, A., Worman, A., and Wrede, S.: How old is streamwater?, open questions in catchment transit time conceptualization, modelling and analysis, Hydrol. Process., 24, 1745–1754, doi:10.1002/hyp.7796, 2010.

HESSD
10, 15871–15914, 2013

McGuire, K. J. and McDonnell, J. J.: A review and evaluation of catchment transit time modeling, J. Hydrol., 330, 543–563, doi:10.1016/j.jhydrol.2006.04.020, 2006.
McGuire, K. J., DeWalle, D. R., and Gburek, W. J.: Evaluation of mean residence time in subsurface waters using oxygen-18 fluctuations during drought conditions in the mid-Appalachians, J. Hydrol., 261, 132–149, doi:10.1016/S0022-1694(02)00006-9, 2002.
McGuire, K. J., Weiler, M., and McDonnell, J. J.: Integrating tracer experiments with modeling to assess runoff processes and water transit times, Adv. Water Resour., 30, 824–837, doi:10.1016/j.advwatres.2006.07.004, 2007.
Mertens, J., Diels, J., Feyen, J., and Vanderborght, J.: Numerical analysis of passive capillary wick samplers prior to field installation, Soil Sci. Soc. Am. J., 71, 35–42, doi:10.2136/sssaj2006.0106, 2007.
Munoz-Villers, L. E. and McDonnell, J. J.: Runoff generation in a steep, tropical montane cloud forest catchment on permeable volcanic substrate, Water Resour. Res., 48, W09528, doi:10.1029/2011WR011316, 2012.
Murphy, B. P. and Bowman, D. M. J. S.: What controls the distribution of tropical forest and savanna?, Ecol. Lett., 15, 748–758, doi:10.1111/j.1461-0248.2012.01771.x, 2012.
Plesca, I., Timbe, E., Exbrayat, J.-F., Windhorst, D., Kraft, P., Crespo, P., Vache, K. B., Frede, H.-G., and Breuer, L.: Model intercomparison to explore catchment functioning: results from a remote montane tropical rainforest, Ecol. Model., 239, 3–13, doi:10.1016/j.ecolmodel.2011.05.005, 2012.
Rinaldo, A., Beven, K. J., Bertuzzo, E., Nicotina, L., Davies, J., Fiori, A., Russo, D., and Botter, G.: Catchment travel time distributions and water flow in soils, Water Resour. Res., 47, W07537, doi:10.1029/2011WR010478, 2011.
Rodgers, P., Soulsby, C., and Waldron, S.: Stable isotope tracers as diagnostic tools in upscaling flow path understanding and residence time estimates in a mountainous mesoscale catchment, Hydrol. Process., 19, 2291–2307, doi:10.1002/hyp.5677, 2005.
Rollenbeck, R., Bendix, J., and Fabian, P.: Spatial and temporal dynamics of atmospheric water inputs in tropical mountain forests of South Ecuador, Hydrol. Process., 25, 344–352, doi:10.1002/hyp.7799, 2011.
Rose, T. P., Davisson, M. L., and Criss, R. E.: Isotope hydrology of voluminous cold springs in fractured rock from an active volcanic region, northeastern California, J. Hydrol., 179, 207–236, doi:10.1016/0022-1694(95)02832-3, 1996.

HESSD
10, 15871–15914, 2013

Soulsby, C., Malcolm, R., Helliwell, R., Ferrier, R. C., and Jenkins, A.: Isotope hydrology of the Allt a' Mharcaidh catchment, Cairngorms, Scotland: implications for hydrological pathways and residence times, Hydrol. Process., 14, 747–762, doi:10.1002/(SICI)1099-1085(200003)14:4<747::AID-HYP970>3.0.CO;2-0, 2000.

Soulsby, C., Tetzlaff, D., and Hrachowitz, M.: Tracers and transit times: windows for viewing catchment scale storage?, Hydrol. Process., 23, 3503–3507, doi:10.1002/hyp.7501, 2009.

Speed, M., Tetzlaff, D., Soulsby, C., Hrachowitz, M., and Waldron, S.: Isotopic and geochemical tracers reveal similarities in transit times in contrasting mesoscale catchments, Hydrol. Process., 24, 1211–1224, doi:10.1002/hyp.7593, 2010.

Tetzlaff, D., Malcolm, I. A., and Soulsby, C.: Influence of forestry, environmental change and climatic variability on the hydrology, hydrochemistry and residence times of upland catchments, J. Hydrol., 346, 93–111, doi:10.1016/j.jhydrol.2007.08.016, 2007.

Turner, J., Albrechtsen, H. J., Bonell, M., Duguet, J. P., Harris, B., Meckenstock, R., McGuire, K., Moussa, R., Peters, N., Richnow, H. H., Sherwood-Lollar, B., Uhlenbrook, S., and van Lanen, H.: Future trends in transport and fate of diffuse contaminants in catchments, with special emphasis on stable isotope applications, Hydrol. Process., 20, 205–213, doi:10.1002/hyp.6074, 2006.

Vache, K. B. and McDonnell, J. J.: A process-based rejectionist framework for evaluating catchment runoff model structure, Water Resour. Res., 42, W02409, doi:10.1029/2005WR004247, 2006.

Viville, D., Ladouche, B., and Bariac, T.: Isotope hydrological study of mean transit time in the granitic Strengbach catchment (Vosges massif, France): application of the FlowPC model with modified input function, Hydrol. Process., 20, 1737–1751, doi:10.1002/hyp.5950, 2006.

Weiler, M., McGlynn, B. L., McGuire, K. J., and McDonnell, J. J.: How does rainfall become runoff?, a combined tracer and runoff transfer function approach, Water Resour. Res., 39, 1315–1327, doi:10.1029/2003WR002331, 2003.

Wilcke, W., Yasin, S., Abramowski, U., Valarezo, C., and Zech, W.: Nutrient storage and turnover in organic layers under tropical montane rain forest in Ecuador, Eur. J. Soil Sci., 53, 15–27, doi:10.1046/j.1365-2389.2002.00411.x, 2002.

Willems, P.: A time series tool to support the multi-criteria performance evaluation of rainfall-runoff models, Environ. Model. Softw., 24, 311–321, doi:10.1016/j.envsoft.2008.09.005, 2009.

HESSD
10, 15871–15914, 2013

Windhorst, D., Waltz, T., Timbe, E., Frede, H.-G., and Breuer, L.: Impact of elevation and weather patterns on the isotopic composition of precipitation in a tropical montane rainforest, Hydrol. Earth Syst. Sci., 17, 409–419, doi:10.5194/hess-17-409-2013, 2013.

Wolock, D. M., Fan, J., and Lawrence, G. B.: Effects of basin size on low-flow stream chemistry and subsurface contact time in the Neversink River Watershed, New York, Hydrol. Process., 11, 1273–1286, doi:10.1002/(SICI)1099-1085(199707)11:9<1273:AID-HYP557>3.0.CO;2-S, 1997.

Zimmermann, B., Elsenbeer, H., and De Moraes, J. M.: The influence of land-use changes on soil hydraulic properties: implications for runoff generation, Forest Ecol. Manag., 222, 29–38, doi:10.1016/j.foreco.2005.10.070, 2006.

HESSD
10, 15871–15914, 2013

Table 1. Applied sampling strategy in the San Francisco catchment.

Sample type	Collection method	Sampled since[a]	Site Name	Site code m a.s.l.	Altitude (Weeks)	Samples Number
Rainfall	Collector	Aug 2010	Estación San Francisco	ECSF	1900	99
Main river	Manually	Aug 2010	Planta (outlet)	PL	1725	104
			San Francisco	SF	1825	104
Tributaries	Manually	Aug 2010	Francisco Head	FH	1917	98
			Zurita	QZ	2047	103
			Navidades	QN	2050	104
			Ramon	QR	1726	104
			Pastos	QP	1925	103
			Milagro	QM	1878	104
			Cruces	QR	1978	102
Creeks	Manually	Dec 2010	Pastos tributary	TP	1950	88
			Q3	Q3	1907	88
Springs	Manually	Aug 2010	PL Spring	PLS	1731	98
			SF Spring	SFS	1826	100
			QR Spring	QRS	1900	100
Pastures soil water	Wick-sampler	Nov 2010	Pastos alto[b]	A1/A2/A3	2025	60/58/45
			Pastos medio[b]	B1/B2/B3	1975	70/70/63
			Pastos bajo[b]	C1/C2/C3	1925	67/71/55
Forest soil water	Wick-sampler	Sep 2010	Bosque alto[b]	D1/D2/D3	2000	78/74/62
			Bosque medio[b]	E1/E2/E3	1900	86/80/62
			Bosque bajo[b]	F1/F2/F3	1825	55/53/36

[a] Sampling campaign was completed until mid-Aug 2012.
[b] There are three wick-samplers per site (i.e. A1 = 0.10 m, A2 = 0.25 m and A3 = 0.40 m below surface).

HESSD
10, 15871–15914, 2013

Table 2. Main characteristics of the San Francisco catchment and its tributaries.

Parameter	Units	Outlet	Subcatchment						
		PL	FH	QZ	QN	QR	QP	QM	QC
Catchment physical characteristics									
Drainage area	[km^2]	76.9	34.9	11.2	9.8	4.7	3.4	1.3	0.7
Mean elevation	[m a.s.l.]	2531	2615	2615	2591	2472	2447	2274	2290
Altitude range	[m]	1325	1133	991	975	1424	975	772	516
Mean slope	[%]	63	63	63	60	69	67	57	56
Hydrological parameters									
Discharge	[mm]	2959	2691	–	1291	–	–	3.315	2742
Baseflow	[mm]	2520	2152	–	1044	–	–	2118	2268
	[%]	85.2	80.0	–	80.8	–	–	63.9	82.7
Land use									
Forest	[%]	68	67	72	65	80	63	90	22
Sub-páramo	[%]	21	29	15	17	18	10	9	10
Pasture/Bracken	[%]	9	3	12	16	2	26	1	67
Others	[%]	2	1	1	2	0	1	0	1
Soil type									
Histosols	[%]	74	74	70	71	70	62	57	54
Regosols	[%]	15	15	18	16	18	21	25	24
Cambisols	[%]	7	7	8	8	8	11	13	14
Stagnasols	[%]	4	4	4	5	4	6	5	8

HESSD
10, 15871–15914, 2013

Table 3. Lumped parameter models used for the calculation of the transit time distribution.

Model	Transit time distribution g(τ)	Parameter(s)
Exponential Model (EM)	$\frac{1}{\tau}\exp\left(\frac{-t}{\tau}\right)$	τ
Linear Model (LM)	$\frac{1}{2\tau}$ for $t \le 2\tau$ 0 for $t > 2\tau$	τ
Exponential Piston flow Model (EPM)	$\frac{\eta}{\tau}\exp\left(-\frac{\eta}{\tau}+\eta-1\right)$ for $t \ge \tau(1-\eta^{-1})$ 0 for $t < \tau(1-\eta^{-1})$	τ, η
Linear Piston flow Model (LPM)	$\frac{\eta}{2\tau}$ for $\tau - \frac{\tau}{\eta} \le t \le \tau + \frac{\tau}{\eta}$ 0 for other t	τ, η
Dispersion Model (DM)	$\left(\frac{4\pi D_p t}{\tau}\right)^{-1/2} t^{-1} \exp\left[-\left(1-\frac{t}{\tau}\right)^2\left(\frac{\tau}{4D_p t}\right)\right]$	τ, D_p
Gamma Model (GM)	$\frac{\tau^{\alpha-1}}{\beta^\alpha \Gamma(\alpha)}\exp^{-\tau/\beta}$	α, β
Two Parallel Linear Reservoirs (TPLR)	$\frac{\phi}{\tau_f}\exp\left(-\frac{t}{\tau_f}\right)+\frac{1-\phi}{\tau_s}\exp\left(\frac{-t}{\tau_s}\right)$	τ_f, τ_s, ϕ

HESSD
10, 15871–15914, 2013

Table 4. Main statistical parameters of observed $\delta^{18}O$ and predicted results for soil waters using a LPM distribution function. Statistical parameters of modeled results: RMSE, bias, mean and σ correspond to the best matching value of the objective function NSE. Uncertainty bounds of modeled parameters (τ and η), calculated through Generalized Likelihood Uncertainty Estimation (GLUE) are showed in parenthesis.

Site	Sampling depth	Observed			Modeled $\delta^{18}O$, ‰, VSMOW						
		$\delta^{18}O$, ‰, VSMOW			Mean	σ^a	NSE[a]	RMSE[a]	Bias	τ	η
	m	Mean	N^a	σ^a	‰	‰	–	‰	‰	weeks	–
Pastures transect											
A1	0.10	−6.70	60	3.65	−6.80	3.06	0.87	1.32	−0.099	3.5 (2.8–4.4)	1.40 (0.93–2.23)
A2	0.35	−6.79	58	3.33	−6.87	2.46	0.73	1.72	−0.084	5.3 (4.6–6.3)	0.99 (0.90–1.28)
A3	0.60	−7.13	45	3.98	−7.31	3.18	0.86	1.46	−0.181	4.9 (3.6–5.3)	1.11 (0.88–1.37)
B1	0.10	−6.84	70	3.71	−6.91	3.01	0.83	1.52	−0.069	4.7 (3.4–5.1)	1.10 (0.93–1.47)
B2	0.35	−7.03	70	3.41	−7.02	2.71	0.78	1.57	0.007	4.3 (3.9–5.3)	0.98 (0.90–1.33)
B3	0.60	−6.76	63	3.41	−6.77	2.97	0.79	1.54	−0.006	4.5 (3.4–5.2)	1.03 (0.89–1.45)
C1	0.10	−6.65	67	3.66	−6.74	3.15	0.84	1.44	−0.090	3.3 (2.3–4.2)	0.96 (0.87–1.82)
C2	0.35	−7.06	71	3.49	−7.10	3.11	0.87	1.27	−0.043	3.1 (2.7–4.4)	0.89 (0.84–1.55)
C3	0.60	−6.52	55	3.07	−6.53	2.56	0.80	1.36	−0.015	5.4 (4.4–5.8)	1.09 (0.88–1.32)
Forest transect											
D1	0.10	−7.38	78	3.12	−7.26	2.56	0.78	1.44	0.122	5.7 (4.8–6.4)	1.27 (0.97–1.60)
D2	0.35	−7.06	74	2.59	−6.97	2.56	0.78	1.19	0.087	6.8 (5.5–9.2)	1.04 (0.86–1.19)
D3	0.60	−6.80	62	2.75	−6.73	2.56	0.80	1.22	0.062	6.0 (4.8–6.7)	0.99 (0.86–1.28)
E1	0.10	−6.65	86	3.14	−6.58	2.56	0.80	1.40	0.070	5.1 (4.8–6.3)	1.15 (0.93–1.61)
E2	0.35	−6.63	78	2.94	−6.64	2.56	0.78	1.37	−0.016	6.4 (5.7–7.3)	1.01 (0.93–1.45)
E3	0.60	−6.44	62	2.57	−6.48	2.56	0.76	1.24	−0.036	8.3 (7.2–9.2)	1.03 (0.88–1.18)
F1	0.10	−6.75	55	3.16	−6.79	2.56	0.89	1.05	−0.039	4.3 (3.8–5.5)	0.96 (0.87–1.38)
F2	0.35	−6.45	53	3.15	−6.54	2.56	0.89	1.03	−0.089	4.3 (3.7–5.5)	0.94 (0.83–1.58)
F3	0.60	−8.09	36	2.56	−8.05	2.56	0.66	1.46	0.045	6.0 (6.0–7.8)	0.80 (0.76–0.94)

[a] N = number of samples, σ = standard deviation, RMSE = Root Mean Square Error, NSE = Nash–Sutcliffe Efficiency.

HESSD
10, 15871–15914, 2013

Table 5. Main statistical parameters of observed $\delta^{18}O$ and predicted results for surface and spring waters using an EPM distribution function. Statistical parameters of modeled results: RMSE, Bias, Mean and σ correspond to the best matching value of the objective function NSE. Uncertainty bounds of modeled parameters (τ and η), calculated through Generalized Likelihood Uncertainty Estimation (GLUE) are showed in parenthesis.

Site	Drainage area km^2	Outlet altitude m a.s.l.	Recharge altitude m a.s.l.	Observed $\delta^{18}O$, ‰, VSMOW Mean	N	σ^a	Modeled $\delta^{18}O$, ‰, VSMOW Mean ‰	σ^a ‰	NSE –	RMSE ‰	Bias ‰	τ weeks	η –
Stream													
PL	76.93	1725	2488	−8.25	97	0.54	−8.25	0.42	0.56	0.36	0.003	2.0 (1.8–2.2)	1.84 (1.73–1.98)
SF	65.09	1825	2437	−8.12	88	0.56	−8.11	0.43	0.55	0.37	0.001	2.0 (1.9–2.2)	1.85 (1.71–1.97)
Streamwater tributaries													
FH	34.92	1917	2492	−8.28	83	0.55	−8.28	0.42	0.48	0.39	0.000	2.1 (2.0–2.3)	1.84 (1.70–1.93)
QZ	11.25	2047	2565	−8.41	93	0.47	−8.42	0.36	0.55	0.32	−0.004	2.2 (2.1–2.5)	1.72 (1.61–1.82)
QN	9.79	2050	2503	−8.28	92	0.50	−8.28	0.40	0.57	0.33	−0.002	2.1 (2.0–2.3)	1.78 (1.67–1.90)
QR	4.66	1726	2350	−7.96	97	0.48	−7.96	0.16	0.56	0.32	0.000	2.2 (2.0–2.4)	1.73 (1.62–1.84)
QP	3.42	1925	2418	−8.07	98	0.34	−8.07	0.26	0.57	0.22	−0.001	3.7 (3.5–4.1)	2.06 (1.91–2.21)
QM	1.29	1878	2310	−7.81	90	0.59	−7.81	0.44	0.51	0.41	0.005	2.0 (1.8–2.2)	1.85 (1.73–1.98)
QC	0.70	1978	2197	−7.62	95	0.30	−7.62	0.24	0.58	0.19	0.000	3.9 (3.8–4.4)	1.97 (1.81–2.06)
Creeks													
TP	0.14	1950	2213	−7.66	80	0.25	−7.66	0.20	0.49	0.17	0.000	4.5 (4.2–5.1)	1.74 (1.61–1.82)
Q3	0.10	1907	2165	−7.67	88	0.54	−7.67	0.45	0.65	0.32	−0.002	2.1 (1.9–2.2)	1.84 (1.72–2.01)
Springs													
PLS	–	1731	2377	−8.03	101	0.50	−8.04	0.43	0.69	0.28	−0.009	2.0 (1.9–2.2)	1.85 (1.70–1.94)
SFS	–	1826	2187	−7.61	101	0.29	−7.61	0.23	0.47	0.21	−0.002	3.3 (3.0–3.6)	1.42 (1.36–1.47)
QRS	–	1900	2285	−7.80	97	0.17	−7.79	0.09	0.28	0.14	0.005	9.6 (8.8–10.1)	1.70 (1.65–1.82)

[a] N = number of samples, σ = standard deviation, RMSE = Root Mean Square Error, NSE = Nash–Sutcliffe Efficiency.

HESSD
10, 15871–15914, 2013

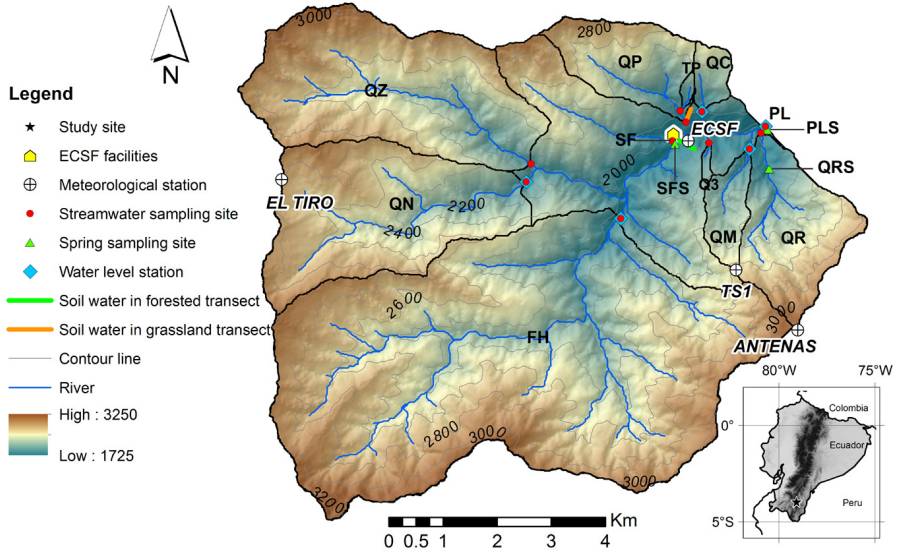

Fig. 1. San Francisco catchment with sampling locations and delineation of drainage area. Acronyms in bold are defined in Table 1. Isotope rainfall sampling was conducted at ECSF facilities.

HESSD
10, 15871–15914, 2013

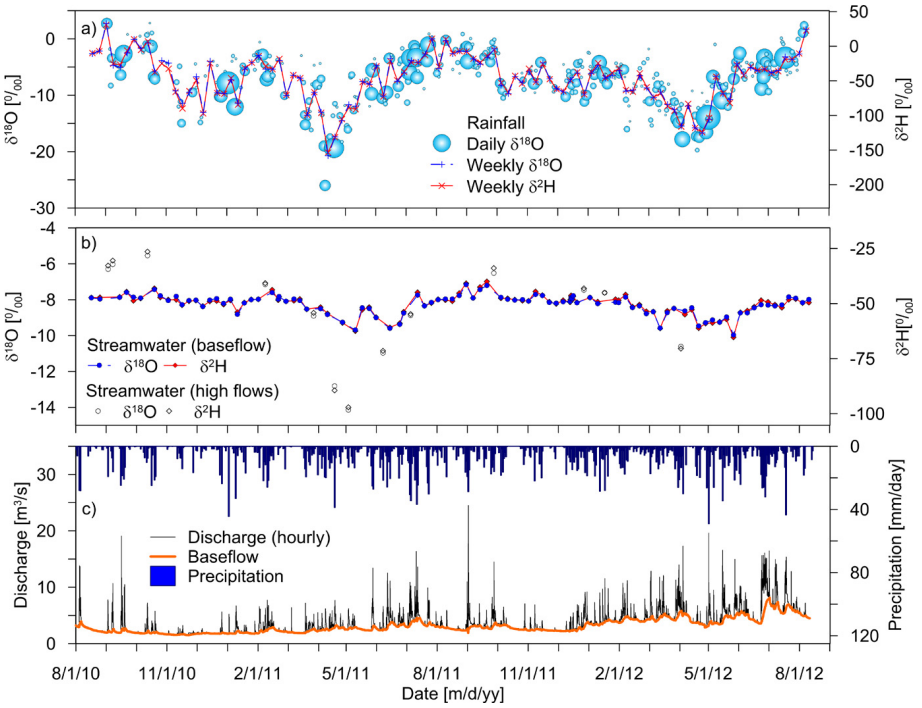

Fig. 2. (a) Weekly δ^{18}O and δ^{2}H at the ECSF rainfall sampling collector; light blue bubbles indicate daily δ^{18}O and relative volume of daily rainfall; **(b)** weekly δ^{18}O and δ^{2}H of streamwater at catchment's main outlet (PL) for baseflow and high flow conditions; and **(c)** time series of rainfall for ECSF meteorological station, hourly discharge and baseflows at the catchment outlet (PL).

HESSD
10, 15871–15914, 2013

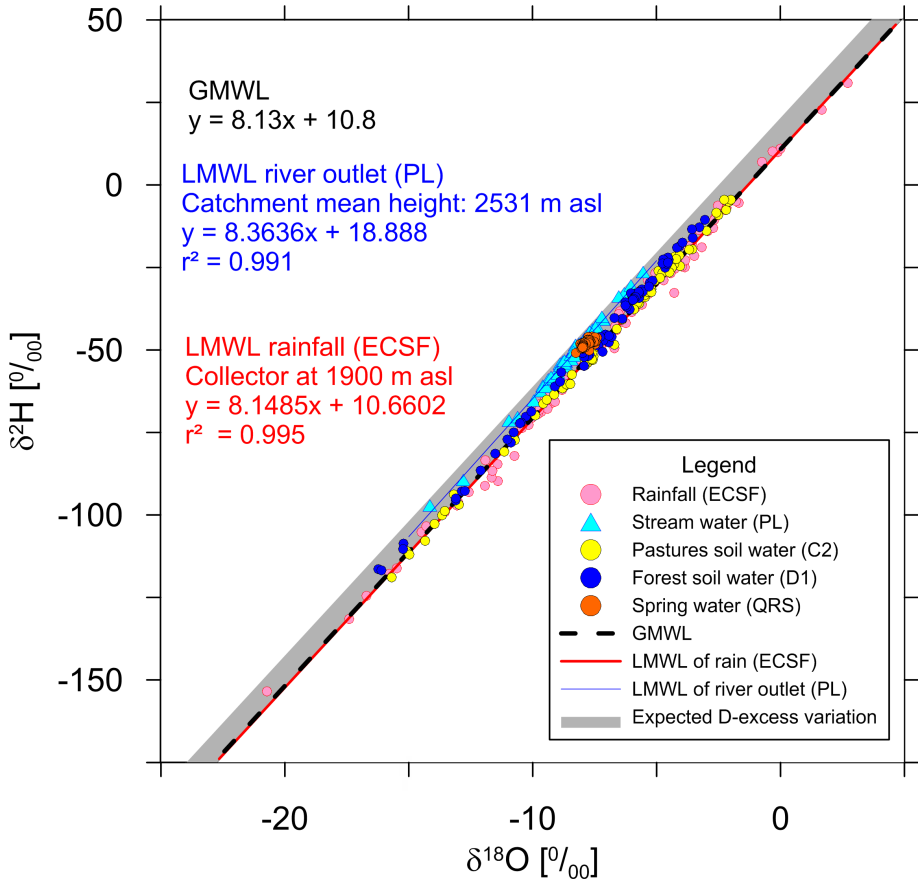

Fig. 3. Shaded area depicts the expected variation range of the Local Meteorological Water Line of rainfall (LMWL) considering the altitudinal range of the catchment (1725–3150 m a.s.l.) and estimated d-excess gradient. Symbols in colors depict weekly values of some of the catchment's waters. Acronyms are defined in Table 1.

HESSD
10, 15871–15914, 2013

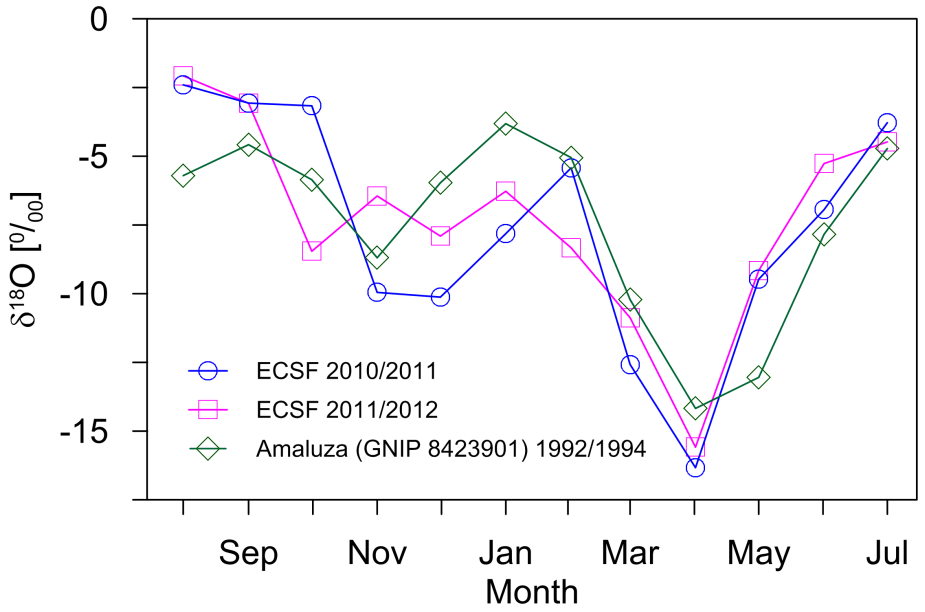

Fig. 4. Monthly isotopic $\delta^{18}O$ signals between two consecutive years (2010–2012) at ECSF (1900 m a.s.l.) and averaged monthly values (1992–1994) at Amaluza GNIP station (latitude −2.61, longitude −78.57, altitude 2378 m a.s.l.).

HESSD
10, 15871–15914, 2013

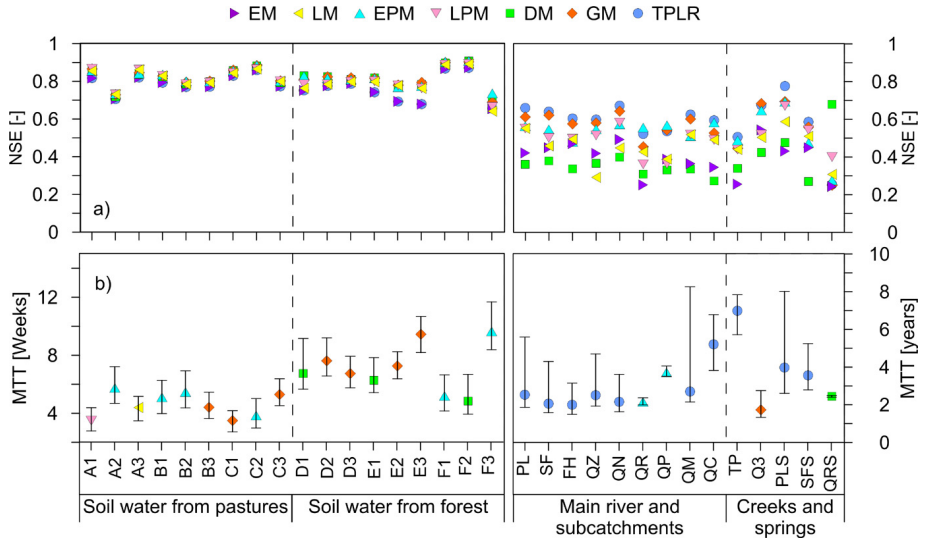

Fig. 5. (a) Best NSE for each of the seven lumped parameter models; **(b)** MTT estimation according the best NSE per site: symbols represent MTT corresponding to the best matching result among 7 models considering the NSE criteria showed in **(a)**, vertical line represents uncertainty bounds according the GLUE methodology for the selected model.

HESSD
10, 15871–15914, 2013

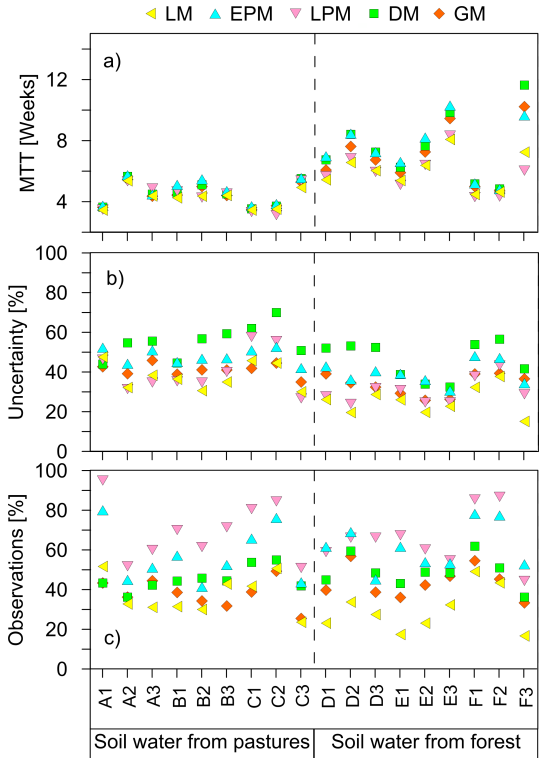

Fig. 6. Intercomparison of models for soil sites according to their: **(a)** estimated mean transit times; **(b)** uncertainty ranges expressed in percentage of its respective MTT estimation; and **(c)** number of observations inside the range of behavioral solutions.

HESSD
10, 15871–15914, 2013

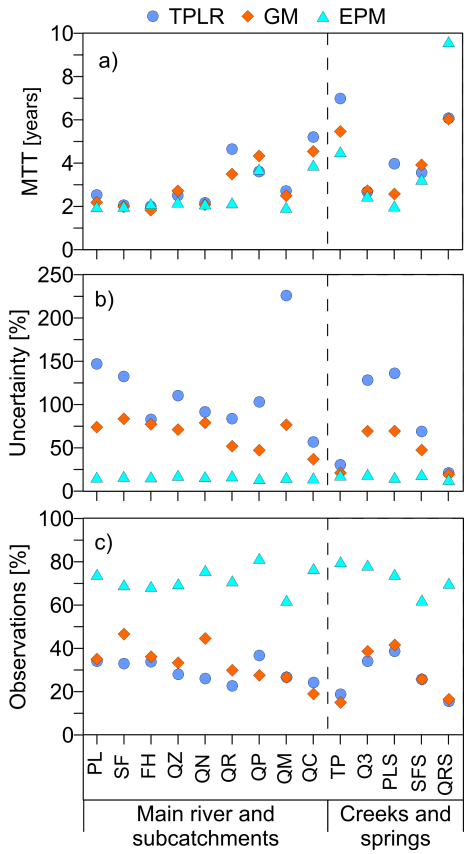

Fig. 7. Intercomparison of models for surface waters and springs according to their: **(a)** estimated mean transit times; **(b)** uncertainty ranges expressed in percentage of its respective MTT estimation; and **(c)** number of observations inside the range of behavioral solutions.

HESSD
10, 15871–15914, 2013

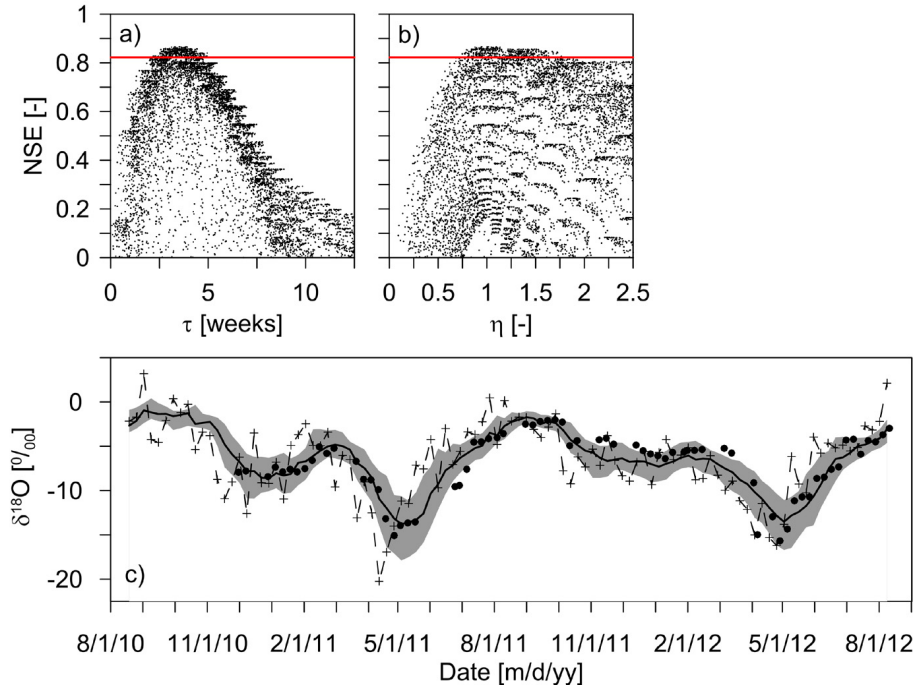

Fig. 8. Fitted results of the LPM model compared to observed data for soil water of a pastures site (C2). Sub-plots **(a)** and **(b)** show the uncertainty analysis of 10 000 simulations and the feasible range of behavioral solutions of model parameters as a 5 % of the top best prediction. Black filled circles in sub-plot **(c)** represents the observed data; the black line and the shaded area represent the best possible solution and its range of variation according to the 5–95 % confidence limits of the behavioral solutions shown in **(a)**; and the gray dashed line with crosses represents the weekly rainfall variation as input function for the model.

HESSD
10, 15871–15914, 2013

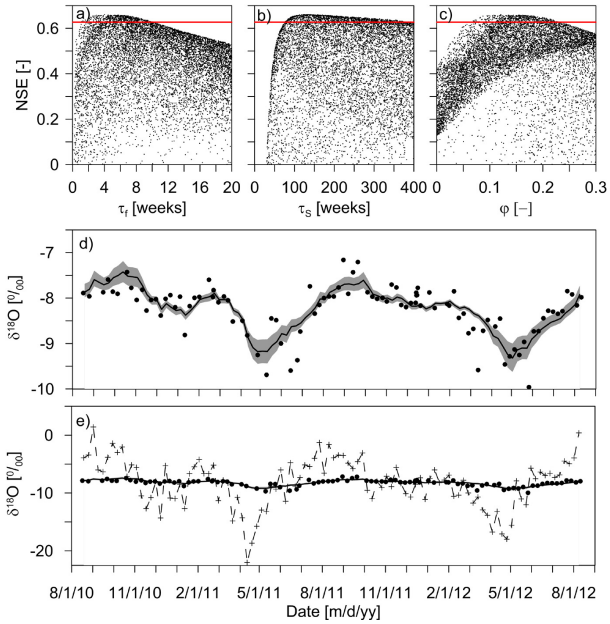

Fig. 9. Uncertainty ranges for outlet stream water (PL site) using a TPLR distribution function. Sub-plots **(a)**, **(b)** and **(c)** show the modeled parameter uncertainties of 10 000 random simulations and the feasible range of behavioral solutions taking a lower limit of 5 % from the best solution. Black filled circles in the sub-plots **(d)** and **(e)** represents the observed data, the black line and shaded area depict the best possible solution and its range of variation according to the 5–95 % confidence limits of the behavioral solutions shown in sub-plot **(b)**; and the gray dashed line with crosses in sub-plot **(e)** represents the weekly rainfall variation as input function for the model.

HESSD
10, 15871–15914, 2013

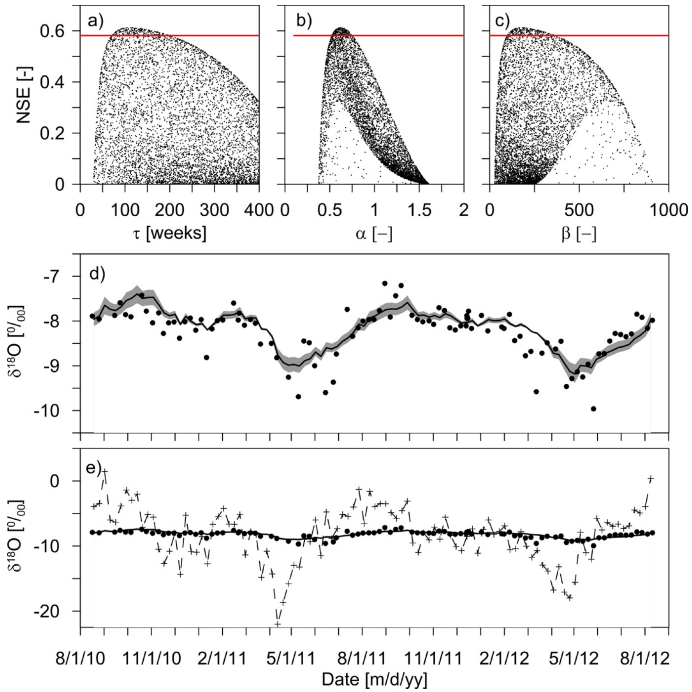

Fig. 10. Uncertainty ranges for outlet stream water (PL site) using a GM distribution function. Sub-plots **(a)**, **(b)** and **(c)** show the modeled parameters uncertainties of 10 000 simulations and the feasible range of behavioral solutions taking a lower limit of 5 % from the best solution. Black filled circles in the sub-plots **(d)** and **(e)** represents the observed data, the black line and the shaded area represent the best possible solution and its range of variation according to the 5–95 % confidence limits of the behavioral solutions shown in sub-plot **(a)**; and the gray dashed line with crosses in sub-plot **(e)** represents the weekly rainfall variation as input function for the model.

HESSD
10, 15871–15914, 2013

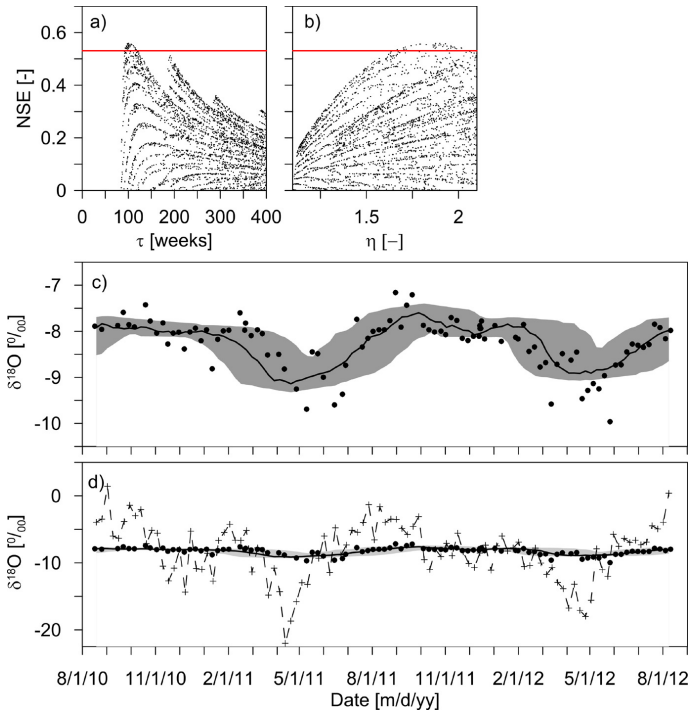

Fig. 11. Uncertainty ranges for outlet stream water (PL site) using an EPM distribution function. Sub-plots **(a)** and **(b)** show the modeled parameters uncertainties of 10 000 simulations and the feasible range of behavioral solutions taking a lower limit of 5 % from the best solution. Black filled circles in the sub-plots **(c)** and **(d)** represent the observed data, the black line and the shaded area represent the best possible solution and its range of variation according the 5–95 % confidence limits of the behavioral solutions shown in sub-plot **(a)**; and the gray dashed line with crosses in sub-plot **(d)** represents the weekly rainfall variation as input function for the model.

HESSD
10, 15871–15914, 2013